



Universiteit
Leiden

The Netherlands

The unique procoagulant adaptations of *pseudonaja textilis* venom factor V and factor X

Schreuder, M.

Citation

Schreuder, M. (2022, September 22). *The unique procoagulant adaptations of pseudonaja textilis venom factor V and factor X*. Retrieved from <https://hdl.handle.net/1887/3464432>

Version: Publisher's Version

License: [Licence agreement concerning inclusion of doctoral thesis in the Institutional Repository of the University of Leiden](#)

Downloaded from: <https://hdl.handle.net/1887/3464432>

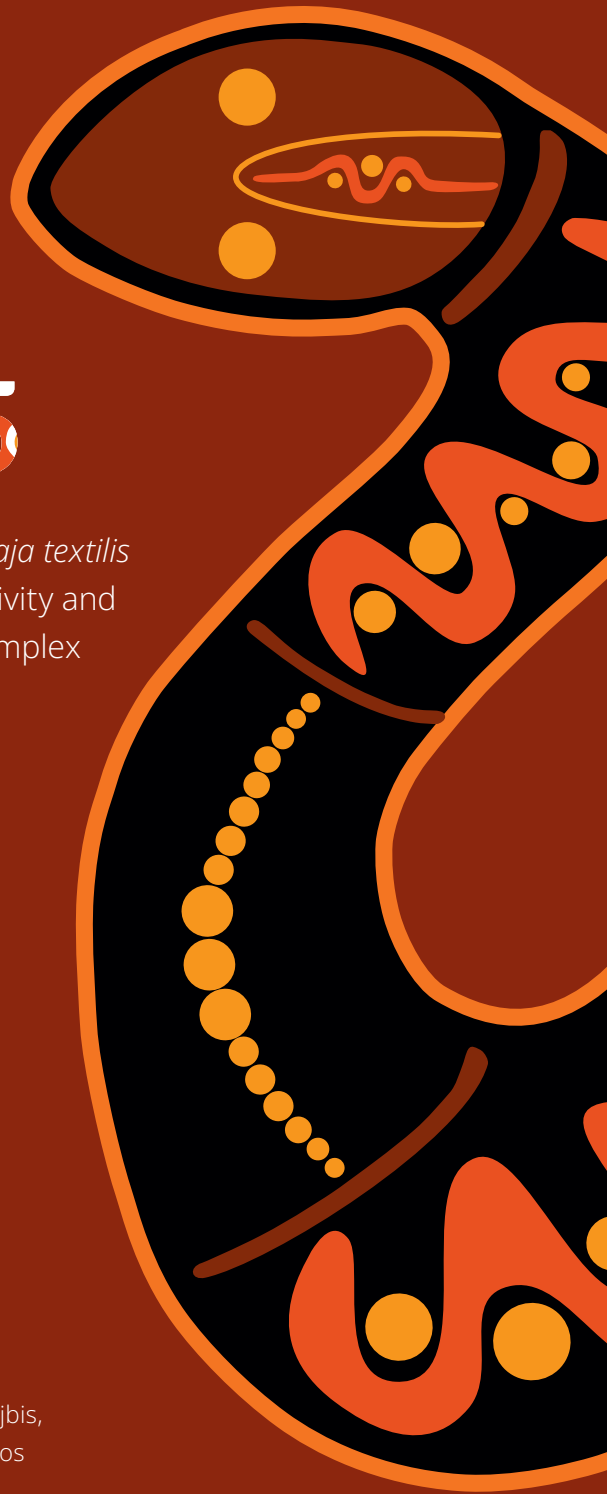
Note: To cite this publication please use the final published version (if applicable).

Chapter 5

Evolutionary Adaptations in *Pseudonaja textilis*
Venom Factor X induce Zymogen Activity and
Resistance to the Intrinsic Tenase Complex

Mark Schreuder, Geraldine Poenou, Viola J.F. Strijbis,
Ka Lei Cheung, Pieter H. Reitsma, Mettine H.A. Bos

Thrombosis and Haemostasis. 2020 120(11):1512-1523





Abstract

The venom of the Australian snake *Pseudonaja textilis* comprises powerful prothrombin activators consisting of factor X (v-ptFX)- and factor V-like proteins. While all vertebrate liver-expressed factor X (FX) homologs, including that of *Pseudonaja textilis*, comprise an activation peptide of ~45-65 residues, the activation peptide of v-ptFX is significantly shortened to 27 residues. In this study, we demonstrate that exchanging the human FX activation peptide for the snake venom ortholog impedes proteolytic cleavage by the intrinsic factor VIIIa-factor IXa tenase complex. Furthermore, our findings indicate that the human FX activation peptide comprises an essential binding site for the intrinsic tenase complex. Conversely, incorporation of factor X into the extrinsic tissue factor-factor VIIa tenase complex is completely dependent on exosite-mediated interactions. Remarkably, the shortened activation peptide allows for factor V-dependent prothrombin conversion while in zymogen-state. This indicates that the active site of FX molecules comprising the v-ptFX activation peptide partially matures upon assembly into a premature prothrombinase complex. Taken together, the shortened activation peptide is one of the remarkable characteristics of v-ptFX that has been modified from its original, thereby transforming FX into a powerful procoagulant protein. Moreover, these results shed new light on the structural requirements for serine protease activation and indicate that catalytic activity can be obtained without formation of the characteristic Ile¹⁶-Asp¹⁹⁴ salt bridge via modification of the activation peptide.

Introduction

Coagulation factor X (FX) is a vitamin K-dependent protein that circulates as an inactive zymogen precursor and is composed of a heavy and light chain that are covalently linked via a disulfide bond. The N-terminal light chain comprises a γ -carboxyglutamic acid-containing domain that is responsible for anionic phospholipid binding and two epidermal growth factor-like domains that have been implicated in macromolecular interactions¹. The C-terminal heavy chain consists of an activation peptide and the serine protease domain that comprises the active site, which is hallmarked by the catalytic triad residues His⁹⁵, Asp¹⁰², and Ser¹⁹⁵ (chymotrypsinogen numbering).

Transition from the zymogen to the protease state requires conformational changes in the FX serine protease domain resulting in a functional realignment of the active site and exosite regions². This essential step is tightly regulated by intrinsic (tissue factor (TF) and factor VIIa (FVIIa)) or extrinsic (factors VIIIa (FVIIIa) and IXa (FIXa)) tenase complex-mediated proteolysis of the highly conserved Arg¹⁵-Ile¹⁶ scissile bond, resulting in liberation of the 52-residue activation peptide. The activation peptide is considered to be important for the specificity of the tenase complexes towards FX, with glycosylation of the human FX activation peptide contributing to the cofactor-dependent substrate recognition^{3,4}. The newly formed N-terminus (Ile¹⁶) engages in a salt bridge with active site residue Asp¹⁹⁴ that induces conformational changes leading to maturation of the serine protease domain^{5,6}. The mature protease FXa is capable of interacting with the activated cofactor Va (FVa) in the presence of an anionic phospholipid membrane and calcium ions, thereby forming the prothrombinase complex that rapidly converts prothrombin to thrombin.

Interestingly, the venom of some Australian Elapid snakes comprises powerful prothrombin-activating enzyme complexes consisting of FXa- and FVa-like proteins that are specifically expressed in the venom gland^{7,8}. Due to selective pressure these venom proteins have been evolutionary adapted to disrupt the hemostatic balance in prey animals, resulting in incapacitation of the prey⁸. The catalytic subunit (v-ptFX) shares ~42% sequence homology with mammalian FX and comprises several unique features⁹⁻¹¹, including a 13-residue insertion directly N-terminal from Tyr⁹⁹ that results in an extended 99-loop. Recently, we have reported that insertion of this region into human FX (generating 'FX-A'¹²) not only impairs inhibition by antithrombin and tissue factor pathway inhibitor, but also induces insensitivity towards the direct FXa inhibitors that are now widely used as oral anticoagulants¹². Another striking difference between v-ptFX and mammalian blood coagulation FX is the length of the activation peptide⁹. Intriguingly, while all vertebrate liver-expressed FX homologs, including that of *P.*

*textilis*¹³, comprise an activation peptide of at least 40 residues, the activation peptide of v-ptFX is only 27 residues long.

In the present study we generated and characterized chimeric FX variants in which the activation peptide was exchanged between human FX (hFX) and v-ptFX to examine the functional role of the shortened activation peptide of v-ptFX. Our results demonstrate that this unique structural element encompasses some remarkable characteristics that significantly impact the procoagulant activity of v-ptFX. These findings thereby highlight the ability of selective pressure to develop unique biologic properties and further show how evolutionary adaptations can improve our understanding of protein biology.

Materials and Methods

Materials: Apixaban was from Alsachim (Illkirch, France). The inhibitor dansylarginine-N-(3-ethyl-1,5-pentanediy)amide (DAPA) and corn trypsin inhibitor (CTI) were from Haematologic Technologies (Essex Junction, VT). 4-amidinophenylmethanesulfonyl fluoride hydrochloride (APMSF) was from Sigma. The peptidyl substrate methoxycarbonylcyclohexylglycylglycyl-Arg-pNA (SpecXa) was from Sekisui Diagnostics (Stamford, CT, USA); the peptidyl substrates N- α -benzyloxycarbonyl-D-Arg-Gly-Arg-pNA (S2765) and H-D-Phe-Pip-Arg-pNA (S2238) were from Instrumentation Laboratories (Bedford, MA, USA). All tissue culture reagents were from Life Technologies (Carlsbad, CA, USA). Calibrator and fluorescent substrate (FluCa) were from Thrombinoscope (Maastricht, the Netherlands). Small unilamellar phospholipid vesicles (PCPS) composed of 75% (wt/wt) hen egg L-phosphatidylcholine (PC) and 25% (wt/wt) porcine brain L-phosphatidylserine (PS) (Avanti Polar Lipids, Alabaster, AL, USA) were prepared and characterized as described previously¹⁴. FX-depleted human plasma, Neoplastine CI Plus 10 prothrombin time (PT) reagent, TriniCLOT automated activated partial thromboplastin time (aPTT) reagent, and substrate buffer (FluCa) were from Diagnostica Stago (Paris, France). Normal pooled plasma (NPP) was from Sanquin (Amsterdam, the Netherlands). All functional assays were performed in HEPES-buffered saline (HBS: 20 mM HEPES, 0.15 M NaCl, pH 7.5) supplemented with 5 mM CaCl₂, 0.1% PEG8000 and filtered over an 0.2 μ m filter (assay buffer).

Proteins: The proteins hFX-R15Q and hFXa-S195A were gifted by Dr. Camire (Children's Hospital of Philadelphia, Philadelphia, United States). Tissue factor pathway inhibitor (TFPI) was a gift from Dr. van 't Veer (Amsterdam University Medical Centers, Amsterdam, The Netherlands). The human plasma-derived coagulation proteins FVIIa, FIXa, factor XIa (FXIa), prothrombin, α -thrombin, antithrombin, and RVV-X were from Haematologic Technologies (Essex Junction, VT, USA). NovoEight was from Novo Nordisk

(Plainsboro, NJ, USA). Human tissue factor (TF, Innovin) was from Siemens (Newark, NY, USA), and recombinant hirudin was from Hyphen Biomed (Neuville-sur-Oise, France). Recombinant wild-type human factor X (hFX) and venom-derived *Pseudonaja textilis* FX and FXa (v-ptFX and v-ptFXa) were prepared, purified, and characterized as described¹⁵. Recombinant constitutively active B-domainless human factor V (FV-810; hFV) and venom-derived *P. textilis* FV (v-ptFV) were prepared, purified, and characterized as described^{12,16}. The extinction coefficients ($E_{0.1\%, 280\text{ nm}}$) of the newly generated hFX-ptAP and ptFX-hAP variants were assumed to be similar to hFX and v-ptFX (1.16)^{16,17}. The molecular weights of the various proteins used were taken as follows: hFX 58.0 kDa; hFX-ptAP 55.0 kDa; v-ptFX 55.0 kDa; ptFX-hAP 58 kDa.

Construction and Purification of FX Variants: Plasmid constructs encoding the chimeric FX variants were prepared from the pCMV4 vector carrying wild-type hFX or v-ptFX. Inserts encoding for the human or *P. textilis* FX activation peptide were synthesized and subcloned into the pCMV4 FX vectors using either BstBI and KasI (hFX-ptAP) or BstEII and BstBI (ptFX-hAP) by Genscript (Piscataway, NJ, USA). Transfection of the plasmids encoding the FX constructs into HEK293 cells, stable clone selection, and the expression and purification of the FX variants were performed as described previously¹². Briefly, FX proteins were purified employing ion-exchange chromatography on a Q-Sepharose FF column (GE Healthcare) using a NaCl elution gradient in TRIS-buffer, pH 7.4. Fractions containing FX activity were pooled and dialyzed versus 20 mM TRIS, 1 mM EDTA, pH 7.0 for 3 hours at 4°C, followed by a two-step dialysis (3 hours and subsequently overnight) versus a 40 mM sodium phosphate buffer, pH 6.8 at 4°C. The dialysate was loaded on a CHT Ceramic Hydroxy Apatite column type I column (Bio-Rad, Hercules, CA, USA) and eluted using a sodium phosphate gradient. Protein purity was assessed by SDS-PAGE analysis using pre-cast 4–12% gradient gels under non-reducing and reducing conditions (50 mM DTT) using the MES buffer system (Life technologies; Carlsbad, CA, USA) followed by staining with Coomassie Brilliant Blue R-250 (CBB).

FX Activation by FVIIa-TF or FIXa-FVIIIa: The rate of FX (9.1 – 2500 nM) activation by the FVIIa-TF complex (FVIIa 0.5 nM; TF 100 nM) was determined in the presence of PCPS (50 μM) in assay buffer at 25 °C. At selected time points, aliquots were taken and quenched in HBS supplemented with 50 mM EDTA. The amidolytic activity of each sample was determined by SpecXa conversion (250 μM), measuring the absorbance at 405 nm and the initial rates of chromogenic substrate hydrolysis were converted to nanomolar of product by reference to a FXa standard curve. The apparent K_m and k_{cat} values for substrate activation were calculated from Michaelis-Menten equations. For FX activation by the FIXa-FVIIIa complex a similar approach was used. FVIII (NovoEight, 40 nM) was activated by thrombin (100 nM) for 30 sec at 25 °C and the reaction was

stopped by the addition of a 10-fold molar excess of hirudin. Immediately thereafter (within 30 sec), the intrinsic tenase complex was assembled by the addition of activated FVIIIa (5 nM) to FIXa (0.5 nM) and PCPS (20 μ M), and the reactions were initiated by the addition of increasing concentrations of zymogen FX (9.1 – 2500 nM) variants. At selected time points, aliquots were taken and quenched, and the amidolytic activity of each sample was determined by SpecXa conversion as described above. The rate of hFX (50 nM) activation by the intrinsic tenase complex (FIXa, 0.5 nM; FVIIIa, 5 nM; PCPS, 50 μ M) was also assessed in the presence of hFX-ptAP or hFX-R15Q (9.1 – 2500 nM), upon which the inhibitory constant (K_i) was determined for inhibition of hFX activation by hFX-ptAP or hFX-R15Q by fitting the data sets to a four-parameter logistic function.

Clotting-based FX Activation Assays. The specific extrinsic clotting activity was determined using a modified FX-specific PT-based assay. Purified FX samples were serially diluted in assay buffer with 0.1% BSA. FX-depleted plasma (45 μ l) was mixed with 5 μ l sample, followed by a 60 s incubation period at 37 °C. Coagulation was initiated by the addition of 50 μ l PT reagent, and the time to fibrin clot formation was monitored using a Start4 coagulation instrument (Diagnostica Stago). The specific intrinsic clotting activity was determined using a modified FX-specific aPTT-based assay. FX samples were serially diluted in assay buffer with 0.1% BSA. FX-depleted plasma (45 μ l) was mixed with sample (5 μ l) and aPTT reagent (50 μ l), followed by an 180 s incubation period at 37 °C. Coagulation was initiated by the addition of 50 μ l of 25 mM CaCl_2 , upon which the time to fibrin clot formation was monitored. Reference curves consisted of serial dilutions of NPP.

Calibrated Automated Thrombography. Thrombin generation was adapted from protocols earlier described¹⁸. Thrombin generation curves were obtained by supplementing FX-depleted plasma with TF (0.5 or 6 pM) or FXIa (0.25 nM), CTI (70 μ g/mL), PCPS (20 μ M), and 10 μ g/mL FX variant. Thrombin formation was initiated by adding substrate buffer (FluCa) to the plasma. The final reaction volume was 120 μ l, of which 80 μ l was plasma. Thrombin formation was determined every 15s for 60min and corrected for the calibrator using Thrombinoscope software.

Prothrombin Activation: Factor X variants (1 μ M) and plasma-derived prothrombin (5.6-20 μ M) were pre-treated with APMSF (100 μ M) and incubated for 60 min at 37 °C in order to allow for the decomposition of unbound inhibitor, thereby preventing interference in the assay¹⁹. Steady-state initial velocities of macromolecular substrate cleavage were determined discontinuously at 25 °C in assay buffer as described¹². Briefly, unless otherwise stated, progress curves of prothrombin were obtained by incubating PCPS (50 μ M), DAPA (10 μ M), prothrombin (1.4 μ M) and FV810 or v-ptFV

(300 nM), and the reaction was initiated with 250 nM of FX, upon which the rate of prothrombin conversion was measured¹².

Assessment of FXa Active Site Maturation: The human FX variants were activated with RVV-X (0.78 µg/mL) for 60 min at 37 °C. Following activation, the kinetics of peptidyl substrate hydrolysis (SpecXa and S2765) by FXa (7.5 nM) were measured in assay buffer upon initiation by the addition of chromogenic substrate (10–800 µM). The rate of inactivation of FXa by antithrombin or apixaban was measured under similar conditions: RVV-X activated FXa variants were incubated at room temperature with apixaban (0.001–100 nM) or antithrombin (0–400 nM) for 10 or 60 min, respectively. Residual FXa activity was assessed by monitoring SpecXa (250 µM) conversion.

Competitive Inhibition of FXa by hFX-ptAP or FXa-S195A: The rate of prothrombinase-assembled FXa inhibition using apixaban, antithrombin, or tissue factor pathway inhibitor (TFPI) was determined in the absence or presence of hFX-ptAP or FXa-S195A, assuming competitive inhibition by FXa and hFX-ptAP/FXa-S195A would occur if the inhibitors are able to bind hFX-ptAP/FXa-S195A. Reaction mixtures (100 µL) in assay buffer contained FXa (1 nM), PCPS (50 µM), FV810 (60 nM) in the absence or presence of hFX-ptAP or FXa-S195A (50 nM). The inhibitors apixaban (0.001–100 nM), antithrombin (0–400 nM), or TFPI (0–10 nM) were added and incubated at room temperature for 10 or 60 min for apixaban/TFPI or antithrombin, respectively. The reaction was initiated with S2765 (100 µM) and the inhibitory constant (K_i) or the half maximal inhibitory concentration (IC_{50}) values were determined by exponential decay function or a four-parameter logistic function, respectively.

Data Analysis: All data are presented as mean ± 1 standard deviation and are the result of at least two to three experiments.

Results

Construction and Expression of FX Variants. Although the activation peptide of FX is poorly conserved throughout vertebrate evolution, the number of amino acids has remained relatively constant (~45–65 residues; **Figure S1**). Sequence alignments have revealed that *P. textilis* liver-expressed FX comprises an activation peptide of similar length (56 residues; **Figure 1A**)¹³. Strikingly, the v-ptFX activation peptide is considerable shorter and consists of 27 residues^{10,11}. As the functional relevance of the shortened activation peptide is unclear, we aimed to examine the role of this structural element by generating two chimeric FX variants. The activation peptide of hFX was exchanged for the corresponding region of v-ptFX and vice versa, thereby creating hFX-ptAP and ptFX-

hAP, respectively (**Figure 1B**). Each variant migrated on SDS-PAGE with the expected mobility (**Figure 1C**). The appearance of the venom FX light chain as a doublet likely results of heterogeneous O-glycosylation¹⁷.

Factor X Activation by the Intrinsic and Extrinsic Tenase Complexes. As tenase-mediated proteolysis of the activation peptide induces the zymogen to protease transition, FX activation by either the intrinsic FVIIIa-FIXa or extrinsic TF-FVIIa tenase complex was functionally assessed. The kinetic parameters for TF-FVIIa-mediated activation of the chimeric variant hFX-ptAP (K_m 332 ± 54 nM, k_{cat} 40 ± 2 s⁻¹) were identical to those of hFX (K_m 349 ± 66 nM, k_{cat} 37 ± 3 s⁻¹) (**Figure 2A**). This demonstrates that introduction of the *P. textilis* venom-derived activation peptide into hFX did not alter the interaction with or cleavage by the extrinsic tenase complex. Furthermore, assessment of the FX activation mediated by the FX activating protease from Russell's viper venom (RVV-X) revealed that RVV-X activated hFX-ptAP in a similar manner to hFX (**Figure S2A**).

Conversely, activation of hFX by the intrinsic FVIIIa-FIXa tenase complex was not detectable following introduction of the venom-derived activation peptide (**Figure 2B**). Moreover, using similar conditions no FXa formation could be detected following incubation of the venom FX derivatives v-ptFX or ptFX-hAP with the human intrinsic or extrinsic tenase complexes (data not shown). Further assessment of the human FX variants demonstrated a nine-fold reduction in the specific intrinsic clotting activity of hFX-ptAP, while its specific extrinsic clotting activity was unperturbed (**Figure 2C**). Additional support for a severe defect in the FVIIIa-FIXa-dependent activation of hFX-ptAP came from thrombin generation analyses in FX-depleted plasma supplemented with plasma concentrations of FX (10 mg/mL) triggered by FXIa (**Figure 2D**) or by a low amount of TF (0.5 pM) (**Figure S2B**). In case of the latter, not only FX but also FIX is activated in the so-called Jossen-loop^{20,21}. These experiments demonstrated an abrogated hFX-ptAP-dependent thrombin generation when coagulation was triggered by FXIa (**Figure 2D**). Furthermore, the thrombin generation was considerably reduced using hFX-ptAP relative to hFX in the presence of a low amount of TF (**Figure S2B**). In contrast, a similar amount of thrombin was generated with hFX or hFX-ptAP following a high TF-trigger (6 pM) that incorporates a larger contribution of FX in the extrinsic pathway (**Figure 2E**).

We made use of a functional competitive assay to examine whether incorporation of the v-ptFX activation peptide reduces binding to the intrinsic tenase complex or induces loss of Arg¹⁵-Ile¹⁶ cleavage site recognition. Our data show that titration of hFX-ptAP into the FVIIIa-FIXa-dependent activation of hFX inhibited the formation of hFXa (K_i 1257 ± 208 nM) (**Figure 2F**). However, hFX-ptAP proved to be a significantly weaker

competitor relative to hFX-R15Q (K_i 105 ± 44 nM), which is a non-activatable FX molecule due to a substitution at the Arg¹⁵ cleavage site in which the human activation peptide is preserved. These results suggest that the activation peptide of hFX comprises an essential binding site for the intrinsic tenase complex, while the extrinsic tenase complex may require various distinct binding regions for substrate recognition²²⁻²⁵.

Prothrombin Conversion by Zymogen FX Variants. *P. textilis* isoform FX, which is thought to be an evolutionary intermediate between liver and venom FX¹³, comprises an activation peptide of identical length and over 90% sequence identity relative to v-ptFX (Figure S1). Previously, isoform FX was reported to display zymogen activity towards the macromolecular substrate prothrombin in conjunction with its cofactor v-ptFX²⁶. To assess whether the shortened *P. textilis* FX activation peptide may contribute to zymogen activity, the zymogen variants were analyzed for their prothrombin conversion activity in a purified component assay using high concentrations of FX and cofactor (FV-810 for human variants and v-ptFV for ptFX variants). Prior to this, all zymogens including prothrombin were separately incubated with 100 μ M APMSF to irreversibly inhibit any active protease, as an up to 0.18 nM FXa activity was observed in the FX protein preparations (Table S1). Control experiments revealed no loss of FX clotting activity as a result of the prolonged incubations with APMSF (Figure S3). In the presence of cofactor and anionic membranes hFX was able to convert considerable amounts of prothrombin over prolonged incubation periods (Figure 3A), corroborating previous findings²⁷. Remarkably, the zymogen FX variants carrying the *P. textilis* activation peptide demonstrated a striking increase in prothrombin conversion relative to hFX, which is reduced following insertion of the human activation peptide (Figure 3A). Kinetic assessments of prothrombin conversion revealed that the FX molecules comprising the snake venom activation peptide exhibited an up to 20-fold enhanced prothrombin activation rate relative to those zymogens carrying the human activation peptide (Figure 3B). Despite this, the overall catalytic rates of prothrombin conversion were approximately five orders of magnitude lower than those observed for prothrombinase-assembled FXa (Table 1), which is consistent with previous findings²⁸. In contrast, macromolecular substrate binding was practically unaffected following exchange of the activation peptides (Table 1). Moreover, the K_m values obtained indicate that in the presence of cofactor-membranes all zymogen variants were able to engage with prothrombin in a manner similar to FXa^{12,17}. Whereas the kinetics of cofactor binding could not be accurately determined for hFX (Figure 3C), the apparent affinity of hFX-ptAP, v-ptFX, and ptFX-hAP for their respective cofactor was ~50-90-fold reduced relative to previously reported values for hFXa or ptFXa (Figure 3C,D, Table 1)^{16,17,29-31}. We further observed that the FX zymogen activity was fully dependent on the presence of the cofactor, as no prothrombin conversion could be detected for zymogen FX-lipids

(data not shown). This is consistent with the fact that the FVa-prothrombin interaction facilitates efficient proteolytic conversion to thrombin³².

To better understand the observed zymogen activity, we next examined the putative contribution of auto-activation or thrombin-mediated activation of zymogen FX. Prolonged incubations of zymogen FX in the presence of cofactor-lipids did not effectuate enzymatic activity towards the peptidyl substrate SpecXa (<0.04% mol/mol FXa) (**Table S1**), suggestive of incomplete maturation of the active site. In addition, no thrombin-mediated proteolysis of the FX heavy chain was observed following SDS-PAGE analysis (**Figure S4A,B**). These results indicate that the *P. textilis* venom-derived activation peptide promotes FX zymogen activity towards the macromolecular substrate in the presence of cofactor only. The cofactor is essential in driving this zymogen-dependent prothrombin conversion, as it mediates productive substrate interactions in the FX serine protease domain resulting in the catalytic conversion of prothrombin.

Competitive Active Site Binding in Zymogen FX. Given that our data suggest that the FX zymogen active site is available for macromolecular substrate engagement and catalysis, we next questioned whether prothrombinase-assembled zymogen FX could be targeted by several active site inhibitors. Since prothrombinase-assembled hFX-ptAP was incapable of SpecXa hydrolysis both in the absence and presence of cofactor-lipids (**Table S1**), we made use of a functional competitive approach and first assessed antithrombin inhibition of purified hFXa in the presence of FV-810 and PCPS. While addition of a 50-fold molar excess of the catalytically inactive FXa variant hFXa-S195A impaired the inhibition of hFXa by antithrombin, no competitive effect was observed upon the addition of hFX-ptAP (**Figure 4A; Table 2**), indicating that antithrombin is unable to bind to prothrombinase-assembled hFX-ptAP. Similar results were obtained for the inhibition of hFXa by apixaban and TFPI (**Figure 4B-C; Table 2**). This indicates that whereas the activation peptide of v-ptFX allows for a cofactor-mediated productive prothrombin interaction, it is incompatible with specific engagement of the active site only. This would provide further support for incomplete maturation of the active site in the FX variants comprising the *P. textilis* activation peptide.

Assessment of Active Site Maturation in FXa Variants. In order to assess whether the activation peptide induces changes in the active site pocket that may further explain the observed zymogen activity, we assessed the active site maturation of FX variants in their protease state (FXa) using several active site probes. In these assays, we focused on the human FXa variants, as ptFXa is highly insensitive to the direct FXa inhibitor apixaban and the macromolecular inhibitor antithrombin^{12,26}. Following RVV-X activation, the hydrolysis rates of SpecXa and S2765 were examined for hFXa and hFXa-ptAP, revealing similar kinetics for both substrates (**Table 3**). Furthermore, titration of the small active

site inhibitor apixaban showed identical IC_{50} values for both protease variants (**Table 3**). In addition, exchange of the activation peptide did not affect inhibition by antithrombin (**Table 3**). Together, these results show that following proteolytic removal of the v-ptFX activation peptide, the conformation of the FXa active site is identical to wild-type FXa.

Discussion

In the current study the functionality of the short activation peptide of venom-derived *P. textilis* FX, v-ptFX, was assessed. Steady state kinetic assessment of intrinsic tenase-mediated FX activation revealed that substitution of the human activation peptide for that of v-ptFX severely impaired intrinsic FX activation, which was hallmarked by a reduction in: i) the k_{cat} , ii) the FX-specific aPTT clotting activity, and iii) thrombin generation following a FXIa or low TF trigger (**Figure 2**). This indicates that the *P. textilis* venom-derived FX activation peptide infers resistance to the human intrinsic tenase complex. Previously, similarly reduced catalytic efficiencies of the intrinsic tenase complex were observed by others who made use of human FX derivatives that lacked most of the activation peptide, but retained the P_1 - P_3 residues Leu¹³-Arg^{154,33}. Employing bovine or human protein components, the absence of the FX activation peptide residues P_4 - P_{52} was demonstrated to result in a lower catalytic rate or K_m , respectively^{4,33}, pointing to an essential role in substrate recognition and catalysis for this region of the human FX activation peptide. While the naturally occurring venom activation peptide assessed in the current study is substantially longer and comprises 27 amino acids, our findings indicate that it does not play a role in substrate recognition and catalysis by the human FVIIIa-FIXa complex. This is because we not only observed a severely reduced catalytic rate of hFX-ptAP activation (**Figure 2B**), but also revealed that hFX-ptAP is a poor competitive inhibitor of hFX activation by the intrinsic tenase complex (**Figure 2F**). Despite this, hFX-ptAP did demonstrate some competition for the intrinsic tenase-mediated hFX activation. This may suggest that FX comprises additional binding sites for intrinsic tenase that are situated outside of the activation peptide, supporting mutagenesis studies which have identified multiple interactive regions in FX^{23,34-36}.

In sharp contrast, steady state kinetic analyses of FX activation by the extrinsic tenase complex yielded comparable kinetic parameters for hFX and hFX-ptAP, indicating that TF-FVIIa binding and cleavage site recognition are not affected upon introduction of the v-ptFX activation peptide (**Figures 1A,S1**). These findings make clear that the human FX activation peptide is not primarily responsible for substrate binding and catalysis, which is supported by earlier studies demonstrating a relatively modest change in kinetic parameters of extrinsic tenase-dependent activation following truncation of the

activation peptide in human FX^{4,37}. As such, these results provide further support for the hypothesis that the substrate-specificity of the extrinsic tenase complex is entirely regulated by distinct regions in the FX heavy and light chains²²⁻²⁵. These data are also consistent with observations in other coagulation protease complexes, indicating that proper presentation and activation of the macromolecular substrates are critically dependent on binding of exosite regions^{38,39}.

Other structural elements that play a role in FX activation are the carbohydrate chains that are present in the FX activation peptide, with the human FX activation peptide comprising two O-linked and two N-linked glycosylation sites⁴⁰. Inhibition studies using the isolated human activation peptide revealed that it interacts with FIXa in a carbohydrate-dependent manner⁴¹. Furthermore, non-specific glycosidase or sialic-acid-binding lectin treatments were shown to inhibit FX activation by both the extrinsic and intrinsic tenase complexes^{42,43}. To specifically explore the contribution of the individual carbohydrates to FX activation, a mutagenesis-based approach was used by Yang *et al.* demonstrating that elimination of the glycosylation sites did not significantly alter the catalytic efficiency of extrinsic tenase⁴. In contrast, removal of the O-linked glycans from the FX activation peptide resulted in a reduced catalytic efficiency of the intrinsic tenase complex⁴. More specifically, the O-glycan at Thr¹⁷ was shown to contribute to intrinsic tenase recognition and binding, while the O-linked carbohydrate at position Thr²⁹ was found to play a role in the stabilization of the FX transition-state intermediate. This indicates that both O-linked carbohydrates make productive interactions with the intrinsic tenase complex. While no experimental data is available on the glycosylation status of the venom FX activation peptide, artificial neural networks predict one N-linked (QNA) and one O-linked carbohydrate (ATL) (**Figure 1A**)^{40,44}. Whether an O-linked carbohydrate is available for productive intrinsic tenase interactions in FX variants comprising the v-ptAP activation peptide remains to be determined.

Using supraphysiological protein concentrations and extended incubation times, all zymogen FX variants demonstrated prothrombin conversion activity in a cofactor-dependent manner (**Figure 3**), albeit at an approximate 10,000-fold lower catalytic rate relative to the FXa protease state (**Table 1**). To ensure that the observed activity was not due to the presence of traces of FXa protease in the protein preparations, the FX variants were preincubated before each assessment with the short-lived non-reversible serine protease inhibitor APMSF. Moreover, the FX zymogen activity was not attributable to cofactor-lipid-mediated auto-activation (**Table S1**) nor to thrombin-mediated FX proteolysis (**Figures S4,S5**). In line with our results, zymogen activity of FX has previously been observed for both human FX and the *P. textilis* isoform FX-ptFV

Pseutarin C-isoform complex^{26,27}. Here we show that the shortened activation peptide of v-ptFX is at the basis of this remarkable characteristic, with the zymogen activity being completely dependent on the presence of the cofactor as no prothrombin conversion could be detected for any of the zymogen FX-lipids without the cofactor present. However, no apparent binding affinity defining the FV-810-zymogen hFX interaction could be determined, suggesting that the $K_{d,app}$ may be in the ~300-500 nM range or higher (**Figure 3C, Table 1**), consistent with data obtained in earlier binding studies². In contrast, all other zymogen FX variants displayed an apparent binding affinity for their respective cofactor that is ~50-90-fold lower in comparison with the human and venom *P. textilis* FXa protease states (**Figure 3C, Table 1**)^{16,17,29-31}. Strikingly, our FX-cofactor complexes bind prothrombin with a similar affinity relative to previously reported values for prothrombinase-assembled FXa^{2,12,45,46}, suggesting that the prothrombin-interactive sites are available in zymogen FX. From this we conclude that the proteolytic activation of FX and subsequent FVa binding might induce structural rearrangements that allow for the maturation of the active site only and enable catalytic activity towards its natural macromolecular substrate, rather than formation of binding sites for substrate recognition. This is consistent with previous observations revealing that FXa binds with a similar affinity to prothrombin in the presence or absence of FVa⁴⁵. Based on our data we propose that the shortened venom FX activation peptide allows for cofactor binding and formation of a premature prothrombinase complex at FX-FVa concentrations that exceed those in plasma but are likely compatible with those found in venom^{1,8}. Perhaps the absence of the acidic/hydrophobic region found in the human activation peptide and/or modified N- or O-linked carbohydrates in the v-ptFX activation peptide might allow for these premature but productive FX-FVa interactions.

The observed zymogen activity may provide v-ptFX with a unique procoagulant gain-of-function that could significantly contribute to its toxic effects once injected into the bloodstream of the prey. However, it is yet to be unequivocally determined whether venom FX is injected in a zymogen or protease form. Protein sequencing of FX peptides derived from the venom of two individual *P. textilis* snakes has failed to identify the activation peptide^{9,11}, suggesting that ptFX exists in a protease state in venom. Similar results have been obtained for homologous venom FX species that require cofactor Va from the host to function and comprise a similarly short activation peptide (*Tropidechus carinatus* and *Hoplocephalus stephensi*; **Figure S1**)^{47,48}. Information on whether the venom glands express proteases that are specialized in the proteolytic removal of the FX activation peptide is lacking thus far. Preservation of the activation peptide may be of relevance for the circulatory survival of venom FX. This because the half-life of human FX is mediated by the two N-linked glycans within the activation peptide, as these protect the protein from clearance⁴⁹. To what extent a similar mechanism

would provide a selective advantage to a venom that is considered to act in a matter of seconds is unclear.

Interestingly, hFX-ptAP displays remarkable similarities to a previously published 'zymogen form' of FXa². In this variant, Ile¹⁶ is substituted for a leucine (FXa-I16L), thereby inducing an equilibrium between a partially and fully matured serine protease that results in a 5- to 15-fold reduced catalytic activity that is fully cofactor-dependent⁵⁰. Furthermore, this variant displayed a longer half-life due to a diminished reactivity with antithrombin and TFPI. Zymogen activity has also been reported for trypsinogen, prothrombin, prethrombin-2, and plasminogen, which is induced via the so-called 'molecular sexuality' mechanism⁵¹⁻⁵⁴. Peptides sequentially similar to the Ile16 N-terminus are able to engage the zymogen's preformed Ile16 cleft⁵¹. In addition, bacterial proteins such as streptokinase, staphylocoagulase, and von Willebrand factor-binding protein comprise an Ile16 N-terminus-like region that is inserted into the zymogen's activation pocket following interaction with the zymogen⁵²⁻⁵⁴. Upon insertion of such N-terminal-like sequences/peptides, the exogenous Ile1 forms a salt bridge with zymogen Asp194. This triggers the zymogen activation, resulting in a conformational change and maturation of the substrate recognition site and oxyanion hole⁵³. Interestingly, other mechanisms may also lead to zymogen activity. For instance, the zymogen tissue type plasminogen activator comprises intrinsic protease activity due to the formation of an intrinsic Lys156-Asp194 salt bridge that promotes an active trypsin-like conformation⁵⁵. Moreover, recent reports have shown that factor XII and prekallikrein are proteolytically active in zymogen form^{56,57}. Although their activity is several orders of magnitude weaker than that of the activated proteases, these findings may indicate a role in the onset of contact activation in intrinsic coagulation. In a similar manner, v-ptFX may initially generate small amounts of thrombin to activate the feedback mechanisms of the coagulation cascade. The subsequent excessive generation of thrombin could lead to venom-induced consumptive coagulopathy (VICC), which is characterized by a (complete) consumption of fibrinogen and factors V and VIII, elevated D- dimer levels, and an international normalized ratio >3^{58,59}. VICC is the most commonly observed clinical envenoming phenotype in humans following a snakebite by the brown snake *P. textilis*⁶⁰. In order to further study the active site maturation in hFX-ptAP, we explored its accessibility for several active site inhibitors using a cofactor-dependent competition assay. None of the ligands were able to engage the active site pocket of hFX-ptAP (**Table 2**). Future studies are therefore required to fully elucidate this remarkable property, which will likely advance our understanding of serine protease biology.

To conclude, we observed that a shortened activation peptide derived from *P. textilis* venom FX infers resistance to intrinsic tenase, thereby confirming that the hFX activation peptide contains a crucial binding site for the intrinsic tenase complex. In addition, v-ptFX has acquired a unique procoagulant gain-of-function as this short activation peptide allows for the formation of productive cofactor interactions and subsequent catalytic activity towards the macromolecular substrate prothrombin while in the zymogen state. As such, these results shed new light on the structural requirements for serine protease activation. Consequently, these data suggest that the characteristic Ile¹⁶-Asp¹⁹⁴ salt bridge is not an essential requirement for serine protease maturation and activity of FX.

Acknowledgements

We gratefully acknowledge Dr. Rodney Camire (Division of Hematology, Department of Pediatrics, Perelman School of Medicine, University of Pennsylvania, USA) for generously providing hFX-R15Q and hFXa-S195A and Dr. Kees van 't Veer for providing TFPI. This work was financially supported by the Bayer Hemophilia Awards Program (Special Project Award) and Landsteiner Foundation for Blood Transfusion (LSBR, grant. no. 1451). The funding agencies had no role in the preparation, review, or approval of the manuscript.

Figures

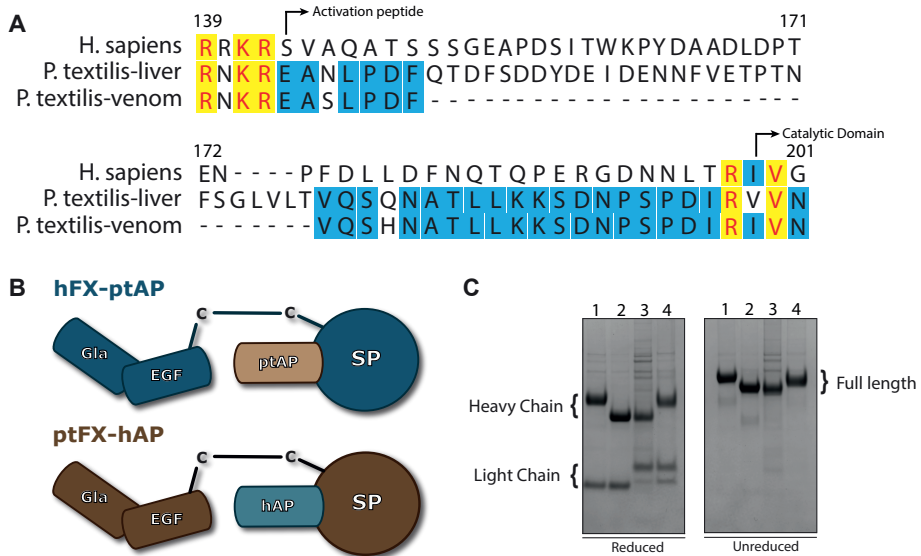


Figure 1. Chimeric factor X variants. (A) Sequence alignment of the activation peptide of human FX (*H. sapiens*), *P. textilil* liver-expressed FX (*P. textilil*-liver), and *P. textilil* venom-expressed FX (*P. textilil*-venom). Residues fully conserved between all three FX species are indicated in yellow; amino acids partially conserved between all of the FX derivatives are indicated in blue. The start of the activation peptide and serine protease domain are indicated; amino acid numbering is according to mature human FX. **(B)** Schematic representation of the chimeric FX variants. The activation peptide was swapped between human FX (blue) and venom-expressed *P. textilil* FX (brown), thereby generating variants hFX-ptAP and ptFX-hAP, respectively. **(C)** SDS-PAGE analysis of purified chimeric FX variants (2 µg/lane) under reducing and non-reducing conditions and visualized by staining with CBB. Lane 1, human FX; lane 2, hFX-ptAP; lane 3, v-ptFX; lane 4, ptFX-hAP. Relevant FX fragments (heavy chain, light chain, or full-length FX) and the apparent molecular weights of the standards are indicated.

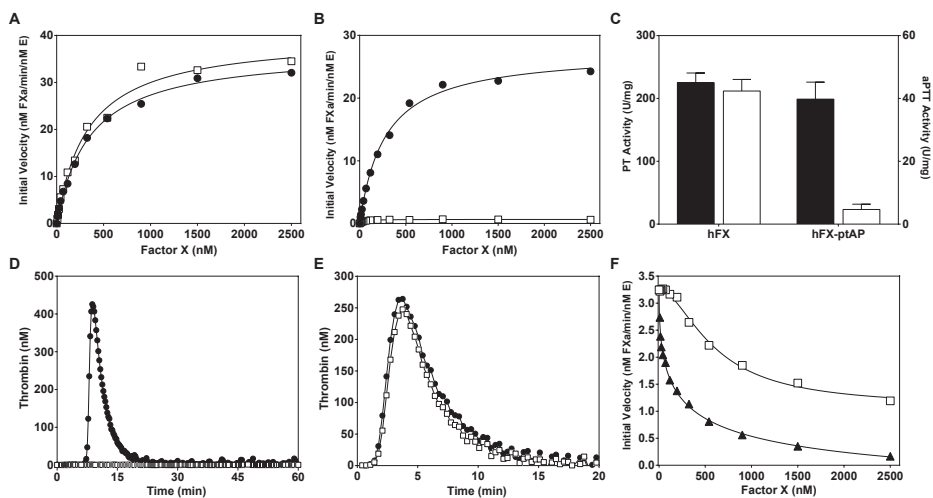


Figure 2. Extrinsic or intrinsic tenase-mediated activation of human factor X variants. The initial velocity of FXa generation was assessed at increasing concentrations of recombinant human FX (hFX) (●) or hFX-ptAP (□) in the presence of 50 μM PCPS and (A) TF (100 nM) and FVIIa (0.5 nM) or (B) FVIIIa (5 nM) and FIXa (0.5 nM). The lines were drawn by fitting the data to the Michaelis-Menten equation using non-linear regression, and the K_m and $k_{cat} \pm 1$ standard deviation of the induced fit were obtained. TF-FVIIa: hFX, K_m 349 ± 143 nM, k_{cat} 37 ± 5 s⁻¹; hFX-ptAP, K_m 332 ± 116 nM, k_{cat} 40 ± 5 s⁻¹. FVIIIa-FIXa: hFX, K_m 275 ± 104 nM, k_{cat} 28 ± 3 s⁻¹. Rates of hFX-ptAP conversion were very low precluding an accurate assessment of kinetic constants. (C) The specific extrinsic (PT Activity; black bars) or intrinsic (aPTT Activity, open bars) clotting activity of FX-deficient plasma supplemented with 1-10 μg/mL hFX or hFX-ptAP was determined as described in 'Materials and Methods'. (D-E) Thrombin generation was measured for 60 min at 37 °C in FX-deficient plasma supplemented with 10 μg/ml hFX (●) or hFX-ptAP (□) in the presence of 0.25 nM FXIa (D) or 6 pM TF (E) and 20 μM PCPS. Thrombin generation was initiated with CaCl₂ and a thrombin fluorogenic substrate as detailed in 'Materials and Methods'. (F) The initial velocity of hFX (50 nM) conversion was determined in the presence of FVIIIa (5 nM), FIXa (0.5 nM), 50 μM PCPS, and increasing concentrations of hFX-ptAP (□) or hFX-R15Q (▲). The lines were drawn by fitting the data to a four-parameter logistic function, and the $K_i \pm 1$ standard deviation of the induced fit were obtained. K_i : hFX-ptAP 1257 ± 208 nM; hFX-R15Q 105 ± 44 nM. Data are representative of two to three independent experiments.

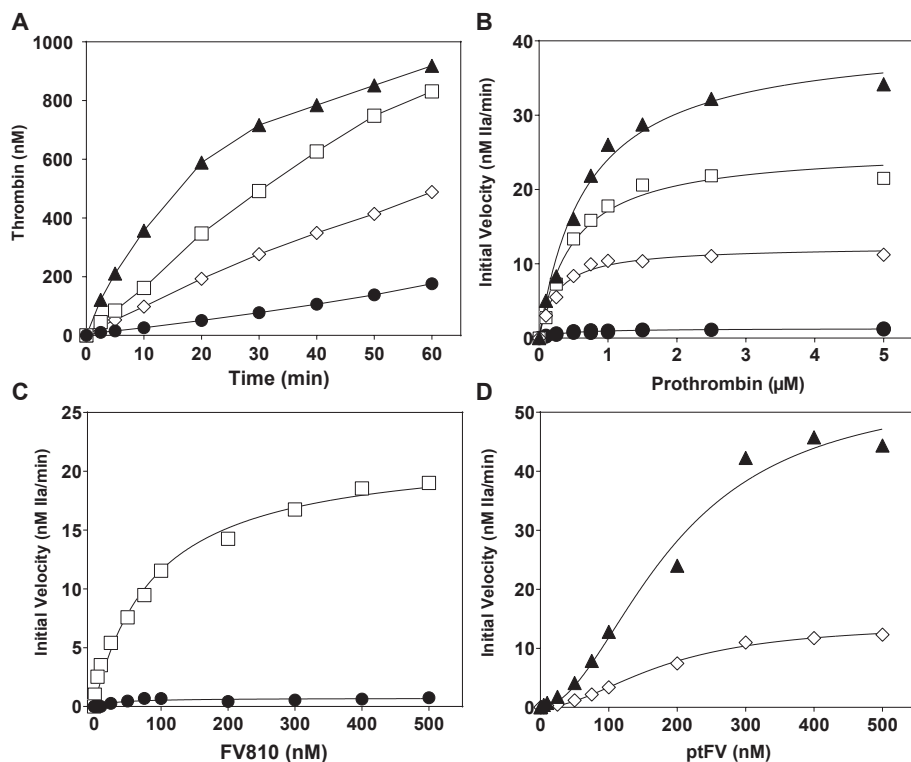


Figure 3. The *P. textilis* activation peptide confers cofactor-dependent zymogen activity. (A) Reaction mixtures containing 1.4 μM prothrombin, 50 μM PCPS, 10 μM DAPA, and 300 nM cofactor (FV-810 for human FX variants or v-ptFV for ptFX variants) were incubated for 5 min at 25 °C. The reaction was initiated with 250 nM FX variant, and thrombin generation was monitored during 60 minutes as described under “Materials and Methods”. SDS-PAGE analysis of the prothrombin conversion by hFX-ptAP and FV-810 under these conditions is shown in **Figure S3**. (B-D) The initial velocity of thrombin formation was determined at increasing concentrations of prothrombin (B), FV-810 (C) or v-ptFV (D) in the presence of 50 μM PCPS and 10 μM DAPA following initiation by 250 nM FX variant, and thrombin generation was monitored during 25 minutes as described under “Materials and Methods”. Prothrombin titrations were performed in the presence of 300 nM cofactor, and FV-810 or v-ptFV titrations were performed with 1.4 μM prothrombin. The symbols represent the following: ● hFX, □ hFX-ptAP, ▲ v-ptFX, ◇ ptFX-hAP. The lines were drawn after analysis of all datasets to a rectangular hyperbola, and the fitted kinetic constants can be found in Table 1. The data are representative of two to three independent experiments.

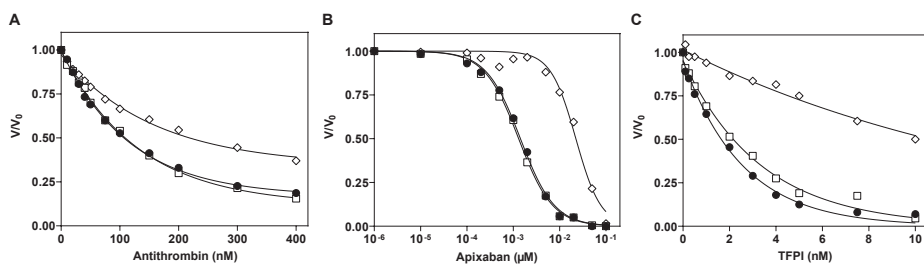


Figure 4. Targeted inhibition of prothrombinase-assembled zymogen factor X. The initial velocity of peptidyl substrate hydrolysis ($100 \mu\text{M}$ S-2765) catalyzed by prothrombinase (1 nM FXa; 60 nM FV-810; $50 \mu\text{M}$ PCPS) in the absence (●) or presence of 50 nM hFX-ptAP (□) or hFXa-S195A (◇) was determined at increasing concentrations of the inhibitors (A) antithrombin, (B) apixaban, or (C) tissue factor pathway inhibitor (TFPI). The data were normalized to the ratio of the velocity at a given concentration (V) over the initial starting velocity (V_0). Data are representative of two to three independent experiments.

	Prothrombin K_m (μM)	Prothrombin k_{cat} (min^{-1})	Cofactor* K_d, app (nM)
hFX	0.36 ± 0.06	N.A. ^a	N.A. ^b
hFX-ptAP	0.49 ± 0.08	0.10 ± 0.003	90 ± 12
v-ptFX	0.69 ± 0.09	0.16 ± 0.007	193 ± 31
ptFX-hAP	0.26 ± 0.04	0.05 ± 0.001	180 ± 12
hFXa	0.51 ± 0.10	933 ± 51	N.A.

Table 1. Kinetic constants for macromolecular substrate conversion by zymogen FX variants. The kinetic constants were obtained as described in 'Materials and Methods'. Fitted values ± 1 standard deviation of the induced fit are representative of two to three independent measurements. N.A., ^aThe k_{cat} value is difficult to estimate because the $K_{d,app}$ between hFX and FV-810 could not be determined. Thus, the total enzyme concentration in this experiment is not known with certainty; the V_{max} was 1.3 ± 0.1 nM min^{-1} . ^bFor this experiment, rates were very low precluding an accurate assessment of apparent binding affinity. *The Va-like cofactor employed was FV-810 for the hFX variants and v-ptFV for the (v-)ptFX variants.

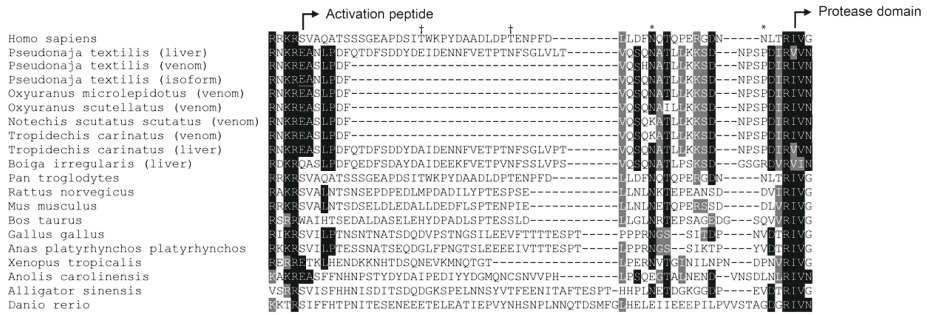
Competitor	Antithrombin K_i (nM)	Apixaban IC_{50} (nM)	TFPI K_i (nM)
No competitor	127 ± 14	1.4 ± 0.2	1.4 ± 0.2
hFX-ptAP	122 ± 8	1.3 ± 0.1	2.3 ± 0.3
hFXa-S195A	260 ± 32	22.4 ± 3.0	10.4 ± 1.5

Table 2. Kinetic parameters for the inhibition of prothrombinase-assembled factor Xa. The kinetic parameters of inhibition were obtained as described in 'Materials and Methods'. Mean values are given ± 1 standard deviation of two to three independent experiments.

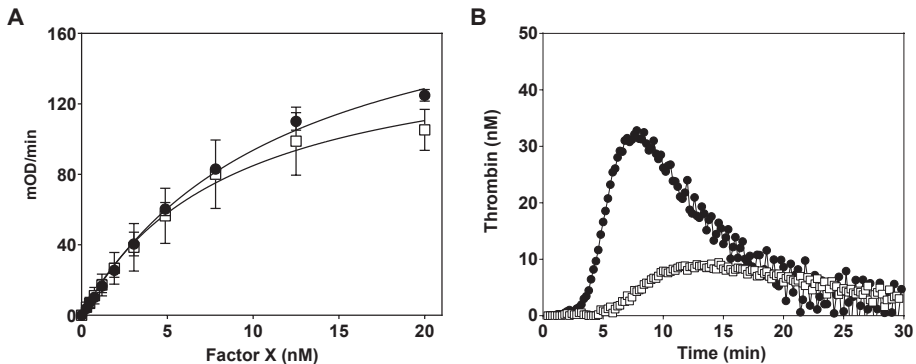
	SpecXa K_m (μM)	SpecXa k_{cat} (min^{-1})	S2765 K_m (μM)	S2765 k_{cat} (min^{-1})	Apixaban IC_{50} (nM)	Antithrombin K_i (nM)
hFXa	92 ± 4	85 ± 1	65 ± 5	80 ± 2	1.5 ± 0.2	80 ± 6
hFXa-ptAP	87 ± 5	73 ± 1	57 ± 5	70 ± 2	1.6 ± 0.2	71 ± 4

Table 3. Assessment of active site maturation. Factor X variants were activated by RVV-X and active site formation was assessed as described in 'Materials and Methods'. Mean values are given ± 1 standard deviation of two to three independent experiments.

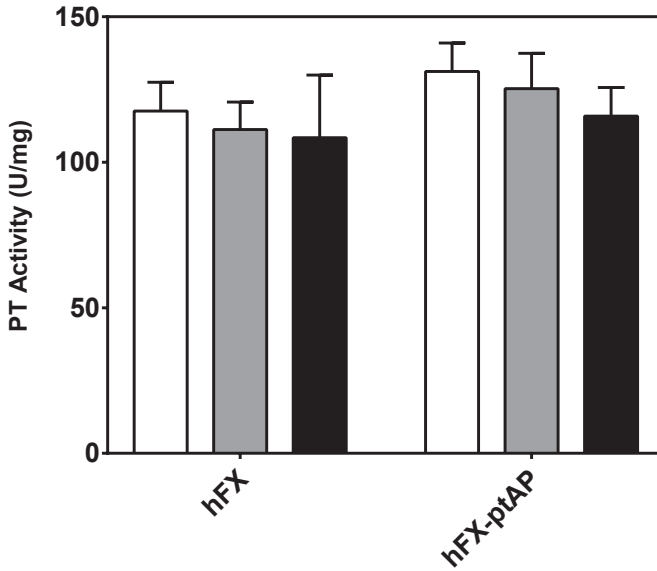
Supplemental Figures



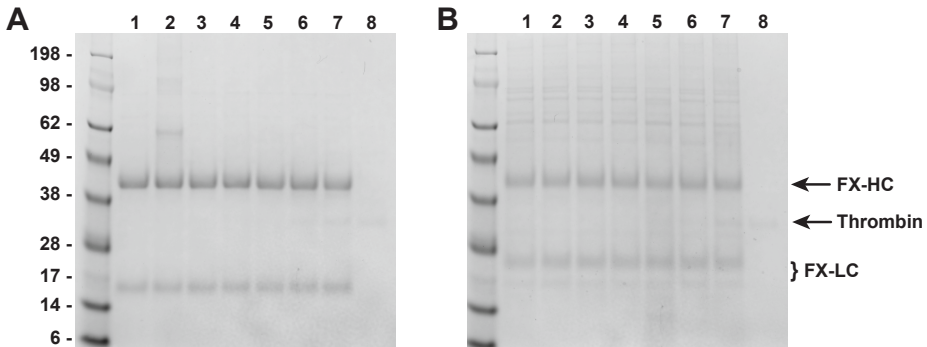
Supplementary figure 1. Alignment of the amino acid sequences comprising the FX activation peptide (Clustal Omega Module; EMBL-EBI, UK). Residues identical to the column consensus are shown in black; residues similar to the column consensus are shown in grey. The start of activation peptide and serine protease domain (Ile16) are indicated. The three-amino acid peptide Arg-Lys-Arg immediately N-terminal to the start of the activation peptide is excised during intracellular processing. The N-linked glycosylation sites Asn181 and Asn191 in human FX are indicated by * and the O-linked glycosylation sites by †(1).



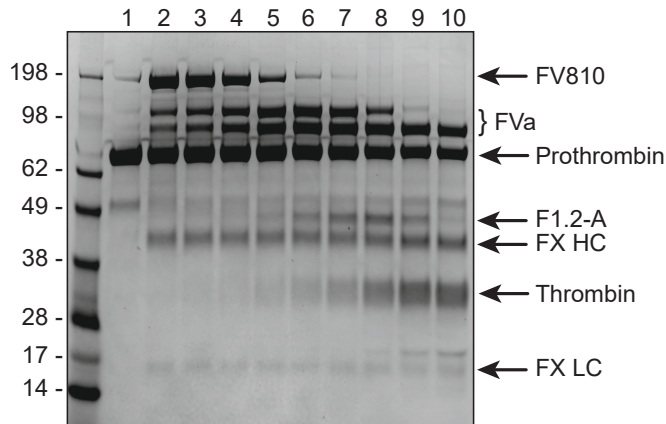
Supplementary figure 2. Activation of human factor X variants by RVV-X or a low TF trigger. (A) The initial velocity of peptidyl substrate hydrolysis (250 μ M SpecXa) was determined at increasing concentrations of hFX (●) or hFX-ptAP (□) in the presence of RVV-X (10 pM). (B) Thrombin generation was measured for 60 min at 37 °C in FX-deficient plasma supplemented with 10 μ g/ml hFX (●) or hFX-ptAP (□) in the presence of 0.5 pM TF and 20 μ M PCPS. Thrombin generation was initiated with CaCl_2 and a thrombin fluorogenic substrate as detailed in 'Materials and Methods'.



Supplementary figure 3. Stability of factor X during APMSF treatment. The specific extrinsic clotting activity (PT Activity) was determined using a modified FX-specific PT-based assay. hFX or hFX-ptAP (1 μ M) were kept on ice (white bars) or were incubated in the absence (grey bars) or presence (black bars) of APMSF (100 μ M) for 60 min at 37 °C. FX variants (1 μ g/mL) were added to FX-deficient plasma and the extrinsic clotting activity was determined as described in ‘Materials and Methods’.



Supplementary figure 4. Thrombin-mediated cleavage of factor X. The recombinant factor X (FX) variants (2500 nM) hFX-ptAP (A) or v-ptFX (B) were incubated with PCPS (50 μ M) and increasing concentrations of thrombin (1-100 nM) in assay buffer for 30 minutes at 37°C. Samples (3 μ g per lane) were subjected to SDS-PAGE under reducing conditions using the MES buffer system and visualized by staining with CBB. Lane 1: FX variant; lanes 2-7: FX variant incubated with 1, 5, 10, 20, 50, or 100 nM thrombin; lane 8: 100 nM thrombin in the absence of FX. Relevant protein bands are indicated; FX-HC, FX heavy chain; FX-LC, factor X light chain. The apparent molecular weights of the standards (kDa) are indicated. The data are representative of two independent experiments.



Supplementary figure 5. Prothrombin cleavage by hFX-ptAP. Plasma-derived prothrombin (1.4 μM) was incubated with 250 nM hFX-ptAP in the presence of FV-810 (300 nM) and PCPS (50 μM) in assay buffer for 1–60 minutes at 25°C. Samples (3 μg per lane) were subjected to SDS-PAGE under reducing conditions using the MES buffer system and visualized by staining with CBB. Lane 1: prothrombin; lanes 2-10: prothrombin incubated for 1, 2.5, 5, 10, 15, 20, 30, 45 or 60 minutes. Relevant protein bands are indicated. F1.2-A, fragment 1.2 (thrombin A chain); FX-HC, factor X heavy chain; FX-LC, factor X light chain. The apparent molecular weights of the standards (kDa) are indicated. The data represents one experiment. The amount of thrombin formed over time is shown in **Figure 3A**.

	Zymogen FX (mOD/min)	Zymogen FX + APMSF (mOD/min)	Zymogen- assembled prothrombinase + APMSF (mOD/min)	FX auto- activation + APMSF (mOD/min)
hFX	0.05 \pm 0.00	0.02 \pm 0.01	N.D.	N.D.
hFX-ptAP	3.31 \pm 0.06	0.03 \pm 0.02	0.19 \pm 0.07	0.06 \pm 0.02
v-ptFX	0.04 \pm 0.01	0.08 \pm 0.08	N.D.	0.13 \pm 0.01
ptFX-hAP	0.05 \pm 0.01	0.00 \pm 0.00	N.D.	N.D.
hFXa (0.1 nM)	2.0 \pm 0.0	N.D.	N.D.	N.D.
hFXa (1 nM)	18.5 \pm 0.1	0.06 \pm 0.00	N.D.	N.D.

Supplementary table 1. Chromogenic activity of recombinant FX variants. The initial velocity of peptidyl substrate hydrolysis (250 μM SpecXa) catalyzed by recombinant zymogen FX variants (250 nM) was determined using non-treated (Zymogen FX) or pre-treatment (Zymogen FX + APMSF) of zymogen FX variants with 100 μM APMSF as described in “Materials and Methods”. The amidolytic activity of hFX-ptAP was also determined in the presence of FV-810 (250 nM), PCPS (50 μM) and SpecXa (250 μM) (zymogen-assembled prothrombinase + APMSF). FX auto-activation was assessed by incubation of APMSF-treated FX (250 nM) with 250 nM cofactor (FV-810 for hFX-ptAP or v-ptFX for v-ptFX) and PCPS (50 μM) at 25 °C for 60 minutes followed by the assessment of FXa activity using peptidyl substrate hydrolysis (250 μM SpecXa). Mean values are given \pm 1 standard deviation of two independent experiments. N.D. indicates not determined.

References

- 1 Bos, M. H. A., Van 't Veer, C. & Reitsma, P. H. Molecular biology and biochemistry of the coagulation factors and pathways of hemostasis. *Williams Hematology* **9th edn.**, 1915–1948 (2016).
- 2 Toso, R., Zhu, H. & Camire, R. M. The conformational switch from the factor X zymogen to protease state mediates exosite expression and prothrombinase assembly. *J Biol Chem* **283**, 18627–18635, doi:10.1074/jbc.M802205200 (2008).
- 3 Rudolph, A. E., Mullane, M. P., Porche-Sorbet, R., Daust, H. A. & Miletich, J. P. The role of the factor X activation peptide: a deletion mutagenesis approach. *Thrombosis and haemostasis* **88**, 756–762 (2002).
- 4 Yang, L., Manithody, C. & Rezaie, A. R. Functional role of O-linked and N-linked glycosylation sites present on the activation peptide of factor X. *J Thromb Haemost* **7**, 1696–1702, doi:10.1111/j.1538-7836.2009.03578.x (2009).
- 5 Huber, R. & Bode, W. Structural Basis of the Activation and Action of Trypsin. *Accounts of Chemical Research* **11**, 114–122 (1978).
- 6 Hedstrom, L. Serine protease mechanism and specificity. *Chem Rev* **102**, 4501–4524 (2002).
- 7 Rao, V. S. & Kini, R. M. Pseutarin C, a prothrombin activator from *Pseudonaja textilis* venom: its structural and functional similarity to mammalian coagulation factor Xa-Va complex. *Thrombosis and haemostasis* **88**, 611–619 (2002).
- 8 Bos, M. H. & Camire, R. M. Procoagulant adaptation of a blood coagulation prothrombinase-like enzyme complex in Australian elapid venom. *Toxins (Basel)* **2**, 1554–1567, doi:10.3390/toxins2061554 (2010).
- 9 Rao, V. S., Swarup, S. & Manjunatha Kini, R. The catalytic subunit of pseutarin C, a group C prothrombin activator from the venom of *Pseudonaja textilis*, is structurally similar to mammalian blood coagulation factor Xa. *Thrombosis and haemostasis* **92**, 509–521, doi:10.1160/TH04-03-0144 (2004).
- 10 Filippovich, I. *et al.* Cloning and functional expression of venom prothrombin activator protease from *Pseudonaja textilis* with whole blood procoagulant activity. *Br J Haematol* **131**, 237–246, doi:10.1111/j.1365-2141.2005.05744.x (2005).
- 11 St Pierre, L. *et al.* Comparative analysis of prothrombin activators from the venom of Australian elapids. *Mol Biol Evol* **22**, 1853–1864, doi:10.1093/molbev/msi181 (2005).
- 12 Verhoef, D. *et al.* Engineered factor Xa variants retain procoagulant activity independent of direct factor Xa inhibitors. *Nat Commun* **8**, 528, doi:10.1038/s41467-017-00647-9 (2017).
- 13 Reza, M. A., Minh Le, T. N., Swarup, S. & Manjunatha Kini, R. Molecular evolution caught in action: gene duplication and evolution of molecular isoforms of prothrombin activators in *Pseudonaja textilis* (brown snake). *J Thromb Haemost* **4**, 1346–1353, doi:10.1111/j.1538-7836.2006.01969.x (2006).
- 14 Higgins, D. L. & Mann, K. G. The interaction of bovine factor V and factor V-derived peptides with phospholipid vesicles. *J Biol Chem* **258**, 6503–6508 (1983).
- 15 Larson, P. J. *et al.* Structure/function analyses of recombinant variants of human factor Xa: factor Xa incorporation into prothrombinase on the thrombin-activated platelet surface is not mimicked by synthetic phospholipid vesicles. *Biochemistry* **37**, 5029–5038, doi:10.1021/bi972428p (1998).
- 16 Toso, R. & Camire, R. M. Removal of B-domain sequences from factor V rather than specific proteolysis underlies the mechanism by which cofactor function is realized. *J Biol Chem* **279**, 21643–21650, doi:10.1074/jbc.M402107200 (2004).

- 17 Bos, M. H. *et al.* Venom factor V from the common brown snake escapes hemostatic regulation through procoagulant adaptations. *Blood* **114**, 686-692, doi:10.1182/blood-2009-02-202663 (2009).
- 18 Hemker, H. C. *et al.* Calibrated automated thrombin generation measurement in clotting plasma. *Pathophysiol Haemost Thromb* **33**, 4-15, doi:10.1159/000071636 (2003).
- 19 Muczynski, V. *et al.* A Thrombin-Activatable Factor X Variant Corrects Hemostasis in a Mouse Model for Hemophilia A. *Thrombosis and haemostasis* **119**, 1981-1993, doi:10.1055/s-0039-1697662 (2019).
- 20 Lu, G., Broze, G. J., Jr. & Krishnaswamy, S. Formation of factors IXa and Xa by the extrinsic pathway: differential regulation by tissue factor pathway inhibitor and antithrombin III. *J Biol Chem* **279**, 17241-17249, doi:10.1074/jbc.M312827200 (2004).
- 21 Zur, M. & Nemerson, Y. Kinetics of factor IX activation via the extrinsic pathway. Dependence of Km on tissue factor. *J Biol Chem* **255**, 5703-5707 (1980).
- 22 Thiec, F., Cherel, G. & Christophe, O. D. Role of the Gla and first epidermal growth factor-like domains of factor X in the prothrombinase and tissue factor-factor VIIa complexes. *J Biol Chem* **278**, 10393-10399, doi:10.1074/jbc.M212144200 (2003).
- 23 Chattopadhyay, A. & Fair, D. S. Molecular recognition in the activation of human blood coagulation factor X. *J Biol Chem* **264**, 11035-11043 (1989).
- 24 Pinotti, M. *et al.* Reduced activation of the Gla19Ala FX variant via the extrinsic coagulation pathway results in symptomatic CRMred FX deficiency. *Thrombosis and haemostasis* **88**, 236-241 (2002).
- 25 Baugh, R. J., Dickinson, C. D., Ruf, W. & Krishnaswamy, S. Exosite interactions determine the affinity of factor X for the extrinsic Xase complex. *J Biol Chem* **275**, 28826-28833, doi:10.1074/jbc.M005266200 (2000).
- 26 Lechtenberg, B. C. *et al.* Crystal structure of the prothrombinase complex from the venom of *Pseudonaja textilis*. *Blood* **122**, 2777-2783, doi:10.1182/blood-2013-06-511733 (2013).
- 27 Estry, D. W. & Tishkoff, G. H. Apparent intrinsic prothrombinase activity of human Factor X zymogen: identification with Factor VIII inhibitor bypassing activity (FEIBA). *Thromb Res* **36**, 549-562, doi:10.1016/0049-3848(84)90194-4 (1984).
- 28 Mann, K. G., Nesheim, M. E., Church, W. R., Haley, P. & Krishnaswamy, S. Surface-dependent reactions of the vitamin K-dependent enzyme complexes. *Blood* **76**, 1-16 (1990).
- 29 Mann, K. G., Nesheim, M. E., Hibbard, L. S. & Tracy, P. B. The role of factor V in the assembly of the prothrombinase complex. *Ann N Y Acad Sci* **370**, 378-388, doi:10.1111/j.1749-6632.1981.tb29750.x (1981).
- 30 Hirbawi, J., Vaughn, J. L., Bukys, M. A., Vos, H. L. & Kalafatis, M. Contribution of amino acid region 659-663 of Factor Va heavy chain to the activity of factor Xa within prothrombinase. *Biochemistry* **49**, 8520-8534, doi:10.1021/bi101097t (2010).
- 31 Bos, M. H. & Camire, R. M. A bipartite autoinhibitory region within the B-domain suppresses function in factor V. *J Biol Chem* **287**, 26342-26351, doi:10.1074/jbc.M112.377168 (2012).
- 32 Schreuder, M., Reitsma, P. H. & Bos, M. H. A. Blood coagulation factor Va's key interactive residues and regions for prothrombinase assembly and prothrombin binding. *J Thromb Haemost* **17**, 1229-1239, doi:10.1111/jth.14487 (2019).
- 33 Duffy, E. J. & Lollar, P. Intrinsic pathway activation of factor X and its activation peptide-deficient derivative, factor Xdes-143-191. *J Biol Chem* **267**, 7821-7827 (1992).
- 34 Chen, L., Manithody, C., Yang, L. & Rezaie, A. R. Zymogenic and enzymatic properties of the 70-80 loop mutants of factor X/Xa. *Protein Sci* **13**, 431-442, doi:10.1110/ps.03406904 (2004).
- 35 Baroni, M. *et al.* Asymmetric processing of mutant factor X Arg386Cys reveals differences between intrinsic and extrinsic pathway activation. *Biochim Biophys Acta* **1854**, 1351-1356, doi:10.1016/j.bbapap.2015.05.012 (2015).

- 36 Vanden Hoek, A. L. *et al.* Coagulation factor X Arg386 specifically affects activation by the intrinsic pathway: a novel patient mutation. *J Thromb Haemost* **10**, 2613-2615, doi:10.1111/jth.12021 (2012).
- 37 Baugh, R. J. & Krishnaswamy, S. Role of the activation peptide domain in human factor X activation by the extrinsic Xase complex. *J Biol Chem* **271**, 16126-16134, doi:10.1074/jbc.271.27.16126 (1996).
- 38 Kumar, A. & Fair, D. S. Specific molecular interaction sites on factor VII involved in factor X activation. *Eur J Biochem* **217**, 509-518 (1993).
- 39 Krishnaswamy, S. Exosite-driven substrate specificity and function in coagulation. *J Thromb Haemost* **3**, 54-67, doi:10.1111/j.1538-7836.2004.01021.x (2005).
- 40 Gupta, R., Jung, E. & Brunak, S. Prediction of N-glycosylation Sites in Human Proteins. **Available online:** <http://www.cbs.dtu.dk/services/NetNGlyc/> (**accessed on April 2018**). (2004).
- 41 Iino, M. *et al.* The role of human factor X activation peptide in activation of factor X by factor IXa. *J Biochem* **116**, 335-340, doi:10.1093/oxfordjournals.jbchem.a124528 (1994).
- 42 Inoue, K. & Morita, T. Identification of O-linked oligosaccharide chains in the activation peptides of blood coagulation factor X. The role of the carbohydrate moieties in the activation of factor X. *Eur J Biochem* **218**, 153-163 (1993).
- 43 Sinha, U. & Wolf, D. L. Carbohydrate residues modulate the activation of coagulation factor X. *J Biol Chem* **268**, 3048-3051 (1993).
- 44 Steentoft, C. *et al.* Precision mapping of the human O-GalNAc glycoproteome through SimpleCell technology. *EMBO J* **32**, 1478-1488, doi:10.1038/emboj.2013.79 (2013).
- 45 Pozzi, N., Chen, Z., Pelc, L. A., Shropshire, D. B. & Di Cera, E. The linker connecting the two kringles plays a key role in prothrombin activation. *Proc Natl Acad Sci U S A* **111**, 7630-7635, doi:10.1073/pnas.1403779111 (2014).
- 46 Ahnstrom, J., Gierula, M., Temenu, J., Laffan, M. A. & Lane, D. A. Partial rescue of naturally occurring active site factor X variants through decreased inhibition by tissue factor pathway inhibitor and antithrombin. *J Thromb Haemost* **18**, 136-150, doi:10.1111/jth.14627 (2020).
- 47 Joseph, J. S., Chung, M. C., Jeyaseelan, K. & Kini, R. M. Amino acid sequence of trocarin, a prothrombin activator from *Tropidechis carinatus* venom: its structural similarity to coagulation factor Xa. *Blood* **94**, 621-631 (1999).
- 48 Rao, V. S., Joseph, J. S. & Kini, R. M. Group D prothrombin activators from snake venom are structural homologues of mammalian blood coagulation factor Xa. *Biochem J* **369**, 635-642, doi:10.1042/BJ20020889 (2003).
- 49 Gueguen, P., Cherel, G., Badirou, I., Denis, C. V. & Christophe, O. D. Two residues in the activation peptide domain contribute to the half-life of factor X in vivo. *J Thromb Haemost* **8**, 1651-1653, doi:10.1111/j.1538-7836.2010.03905.x (2010).
- 50 Bunce, M. W., Toso, R. & Camire, R. M. Zymogen-like factor Xa variants restore thrombin generation and effectively bypass the intrinsic pathway in vitro. *Blood* **117**, 290-298, doi:10.1182/blood-2010-08-300756 (2011).
- 51 Bode, W. & Huber, R. Induction of the bovine trypsinogen-trypsin transition by peptides sequentially similar to the N-terminus of trypsin. *FEBS Lett* **68**, 231-236, doi:10.1016/0014-5793(76)80443-7 (1976).
- 52 Boxrud, P. D., Verhamme, I. M., Fay, W. P. & Bock, P. E. Streptokinase triggers conformational activation of plasminogen through specific interactions of the amino-terminal sequence and stabilizes the active zymogen conformation. *J Biol Chem* **276**, 26084-26089, doi:10.1074/jbc.M101966200 (2001).
- 53 Friedrich, R. *et al.* Staphylocoagulase is a prototype for the mechanism of cofactor-induced zymogen activation. *Nature* **425**, 535-539, doi:10.1038/nature01962 (2003).

- 54 Kroh, H. K., Panizzi, P. & Bock, P. E. Von Willebrand factor-binding protein is a hysteretic conformational activator of prothrombin. *Proc Natl Acad Sci U S A* **106**, 7786-7791, doi:10.1073/pnas.0811750106 (2009).
- 55 Renatus, M. *et al.* Lysine 156 promotes the anomalous proenzyme activity of tPA: X-ray crystal structure of single-chain human tPA. *EMBO J* **16**, 4797-4805, doi:10.1093/emboj/16.16.4797 (1997).
- 56 Ivanov, I. *et al.* Proteolytic properties of single-chain factor XII: a mechanism for triggering contact activation. *Blood* **129**, 1527-1537, doi:10.1182/blood-2016-10-744110 (2017).
- 57 Ivanov, I. *et al.* Protease activity in single-chain prekallikrein. *Blood* **135**, 558-567, doi:10.1182/blood.2019002224 (2020).
- 58 Isbister, G. K. Procoagulant snake toxins: laboratory studies, diagnosis, and understanding snakebite coagulopathy. *Semin Thromb Hemost* **35**, 93-103, doi:10.1055/s-0029-1214152 (2009).
- 59 Masci, P. P., Rowe, E. A., Whitaker, A. N. & de Jersey, J. Fibrinolysis as a feature of disseminated intravascular coagulation (DIC) after *Pseudonaja textilis textilis* envenomation. *Thromb Res* **59**, 859-870, doi:10.1016/0049-3848(90)90399-w (1990).
- 60 Johnston, C. I. *et al.* The Australian Snakebite Project, 2005-2015 (ASP-20). *Med J Aust* **207**, 119-125, doi:10.5694/mja17.00094 (2017).

Supplemental References

1. Hansson K, Stenflo J. Post-translational modifications in proteins involved in blood coagulation. *Journal of thrombosis and haemostasis : JTH* 2005; 3(12): 2633-48.